Published OnlineFirst April 27, 2010; DOI: 10.1158/1535-7163.MCT-09-0986

Research Article

Molecular Cancer Therapeutics

AT7867 Is a Potent and Oral Inhibitor of AKT and p70 S6 Kinase That Induces Pharmacodynamic Changes and Inhibits Human Tumor Xenograft Growth

Kyla M. Grimshaw[1], Lisa-Jane K. Hunter[2], Timothy A. Yap[2], Simon P. Heaton[2], Mike I. Walton[2], Steven J. Woodhead[1], Lynsey Fazal[1], Matthias Reule[1], Thomas G. Davies[1], Lisa C. Seavers[1], Victoria Lock[1], John F. Lyons[1], Neil T. Thompson[1], Paul Workman[2], and Michelle D. Garrett[2]

Abstract

The serine/threonine kinase AKT plays a pivotal role in signal transduction events involved in malignant transformation and chemoresistance and is an attractive target for the development of cancer therapeutics. Fragment-based lead discovery, combined with structure-based drug design, has recently identified AT7867 as a novel and potent inhibitor of both AKT and the downstream kinase p70 S6 kinase (p70S6K) and also of protein kinase A. This ATP-competitive small molecule potently inhibits both AKT and p70S6K activity at the cellular level, as measured by inhibition of GSK3β and S6 ribosomal protein phosphorylation, and also causes growth inhibition in a range of human cancer cell lines as a single agent. Induction of apoptosis was detected by multiple methods in tumor cells following AT7867 treatment. Administration of AT7867 (90 mg/kg p.o. or 20 mg/kg i.p.) to athymic mice implanted with the PTEN-deficient U87MG human glioblastoma xenograft model caused inhibition of phosphorylation of downstream substrates of both AKT and p70S6K and induction of apoptosis, confirming the observations made *in vitro*. These doses of AT7867 also resulted in inhibition of human tumor growth in PTEN-deficient xenograft models. These data suggest that the novel strategy of AKT and p70S6K blockade may have therapeutic value and supports further evaluation of AT7867 as a single-agent anticancer strategy. *Mol Cancer Ther; 9(5); 1100–10. ©2010 AACR.*

Introduction

AKT (also known as protein kinase B) is a serine/threonine kinase that lies downstream of phosphatidylinositol 3-kinase (PI3K) and plays a key role in a range of cellular functions, including cell growth, proliferation, metabolism, and survival (1, 2). Three closely related isoforms of AKT with overlapping cellular functions have been identified, termed AKT1, AKT2, and AKT3 (3).

AKT activation requires the association of its NH_2 terminal pleckstrin homology domain with cell membrane phosphatidylinositol (3,4,5)-trisphosphate produced by PI3K (4). This facilitates phosphorylation of AKT at Thr^{308} and Ser^{473}, both of which are necessary for full activation of the protein. Phosphorylation of Thr^{308} requires phosphoinositide-dependent kinase 1 (5, 6). A number of kinases have been reported to phosphorylate Ser^{473}, the most prominent being the mammalian target of rapamycin complex 2 (7–10). The activation of AKT is antagonized by the tumor suppressor PTEN (phosphatase and tensin homologue on chromosome 10) through the dephosphorylation of phosphatidylinositol (3,4,5)-trisphosphate (11).

There are numerous proteins downstream of AKT which, when phosphorylated, participate in the regulation of critical cellular processes, including growth, proliferation, metabolism, and survival. Those involved in cell growth include p70 S6 kinase (p70S6K), S6 ribosomal protein (S6RP), and the mammalian target of rapamycin complex 1 (12), whereas cell proliferation and metabolism are regulated through GSK3β phosphorylation (13). A number of proapoptotic proteins, including BAD (14), caspase-9 (15), and the forkhead family of transcription factors (16), enable AKT to regulate cell survival. Importantly, negative feedback loops have been described, which link proteins downstream of AKT with those upstream or with AKT itself (17).

Aberrations along the PI3K/AKT pathway have been shown to drive a range of malignancies through mechanisms including activation of upstream receptor tyrosine kinases, *PIK3CA* mutations, *PTEN* mutations, *AKT* amplifications and mutations, and overexpression and hyperactivation of AKT proteins themselves (2, 18–21). Thus, the pharmacologic ablation of AKT activity represents a

Authors' Affiliations: [1]Astex Therapeutics, 436 Cambridge Science Park, Cambridge, United Kingdom and [2]Cancer Research UK Centre for Cancer Therapeutics, Institute of Cancer Research, Haddow Laboratories, Sutton, United Kingdom

Corresponding Author: Michelle D. Garrett, Cancer Research UK Centre for Cancer Therapeutics, Institute of Cancer Research, Haddow Laboratories, 15 Cotswold Road, Sutton, Surrey SM2 5NG, United Kingdom. Phone: 44-20-8722-4352; Fax: 44-20-8722-4126. E-mail: michelle.garrett@icr.ac.uk

doi: 10.1158/1535-7163.MCT-09-0986

Published OnlineFirst April 27, 2010; DOI: 10.1158/1535-7163.MCT-09-0986

rational approach to anticancer therapy. Moreover, PI3K/AKT pathway activation is a frequent hallmark of tumors resistant to treatment with chemotherapy or targeted therapies, such as growth factor inhibitors (22–24). Therefore, AKT inhibition in these tumor types may also have therapeutic value either as monotherapy or in rational combinations with other antitumor agents (25).

Small molecules have been described, which target various vital components of the PI3K/AKT pathway by blocking activation of AKT or its downstream targets (2). These include the PI3K inhibitors LY294002 and wortmannin and, more recently, isoform-specific PI3K inhibitors with differing biological profiles (2, 26, 27). These agents and also drugs such as rapamycin and its analogues that inhibit mTOR are currently progressing through clinical trials in a number of cancer types (28). The latter compounds provide proof of principle that the PI3K-AKT pathway can be successfully targeted for clinical benefit in cancer (2).

A number of compounds which block the activation of AKT through a range of different mechanisms have recently been described, emphasizing the validity and current interest in AKT as an antitumor drug target (2). The inhibition of both AKT and p70S6K with a single agent has not been previously described. Targeting these two key components of the PI3K-AKT pathway through specific vertical inhibition may have therapeutic value.

We have used high-throughput X-ray crystallography and fragment-based lead discovery technologies to identify fragment hits against AKT. These fragments were validated by structural studies and rapidly transformed into potent lead compounds using structure-based design to increase the efficiency of the medicinal chemistry. This research was recently described in detail and has identified potent, low molecular weight inhibitors of AKT that exhibit drug-like properties (29–32).

In this paper, we describe the detailed pharmacologic profile of one of these compounds, AT7867, and also identify this agent as a potent inhibitor of p70S6K in cells. We show that this orally bioavailable small molecule causes appropriate biomarker modulation and apoptosis both *in vitro* and *in vivo* and exhibits antitumor efficacy in human tumor xenograft models.

Materials and Methods

Cell culture and reagents. All cell lines were purchased from the American Type Culture Collection and grown in their recommended culture medium, which was supplemented with 10% fetal bovine serum at 37°C in an atmosphere of 5% CO_2 and passaged for <6 months. All reagents were purchased from Sigma unless otherwise stated. AT7867 (31) and LY294002 (Calbiochem, Merck Biosciences) were dissolved to a 10 mmol/L stock in DMSO, whereas okadaic acid (Calbiochem, Merck Biosciences) was dissolved to a 50 μmol/L stock in DMSO. The recombinant purified AKT2 enzyme used was the pleckstrin homology–truncated AKT2 protein PKB-PIF Pif as previously described (29), which was kindly provided by Professor David Barford (Institute of Cancer Research). GSK3β, histone H1, protein kinase A (PKA) and p70S6K enzymes, phosphorylated glycogen synthase peptide-2, PKA, and p70S6K substrates were purchased from Upstate Biotechnology, whereas protein kinase C and glycogen synthase–derived peptide GS1-8 were from Calbiochem. Cyclin-dependent kinase 2 (CDK2)/cyclin A was prepared in-house at Astex Therapeutics.

In vitro *kinase assays.* Kinase assays for AKT2, PKA, p70S6K, and CDK2/cyclin A were all carried out in a radiometric filter binding format. Assay reactions were set up in the presence of compound. For AKT2, the AKT2 enzyme and 25 μmol/L AKTide-2T peptide (HARKRERTYSFGHHA) were incubated in 20 mmol/L MOPS (pH 7.2), 25 mmol/L β-glycerophosphate, 5 mmol/L EDTA, 15 mmol/L $MgCl_2$, 1 mmol/L sodium orthovanadate, 1 mmol/L DTT, 10 μg/mL bovine serum albumin, and 30 μmol/L ATP (1.16 Ci/mmol) for 4 hours. For PKA, the PKA enzyme and 50 μmol/L peptide (GRTGRRNSI) were incubated in 2 mmol/L MOPS (pH 7.2), 25 mmol/L β-glycerophosphate, 5 mmol/L EDTA, 15 mmol/L $MgCl_2$, 1 mmol/L orthovanadate, 1 mmol/L DTT, and 40 μmol/L ATP (0.88 Ci/mmol) for 20 minutes. For p70S6K, the p70S6K enzyme and 25 μmol/L peptide substrate (AKRRRLSSLRA) were incubated in 10 mmol/L MOPS (pH 7), 0.2 mmol/L EDTA, 1 mmol/L $MgCl_2$, 0.01% β- mercaptoethanol, 0.1 mg/mL bovine serum albumin, 0.001% Brij-35, 0.5% glycerol, and 15 μmol/L ATP (2.3 Ci/mmol) for 60 min. For CDK2, the CDK2/cyclin A enzyme and 0.12 μg/mL histone H1 were incubated in 20 mmol/L MOPS (pH 7.2), 25 mmol/L β-glycerophosphate, 5 mmol/L EDTA, 15 mmol/L $MgCl_2$, 1 mmol/L sodium orthovanadate, 1 mmol/L DTT, 0.1 mg/mL bovine serum albumin, and 45 μmol/L ATP (0.78 Ci/mmol) for 4 hours. Assay reactions were stopped by adding an excess of orthophosphoric acid, and the stopped reaction mixture was then transferred to Millipore MAPH filter plates and filtered. The plates were then washed, scintillant was added, and radioactivity was measured by scintillation counting on a Packard TopCount. IC_{50} values were calculated from replicate curves using GraphPad Prism software. AKT1 and AKT3 enzyme assays were carried out at Invitrogen Ltd., whereas all other enzyme assays were done at Upstate Biotechnology.

Alamar blue cell proliferation assay. Cells were plated in 96-well microplates at 5,000 per well in medium supplemented with 10% fetal bovine serum and grown for 24 hours before treatment with AT7867. Inhibitor or vehicle control was added to the cells for 72 hours. Following this, Alamar Blue solution (BioSource, Nivelle Belgium) was added as stated in the manufacturer's instructions. The IC_{50} value for each inhibitor was calculated in GraphPad Prism using nonlinear regression analysis and a sigmoidal dose-response (variable slope) equation.

Phosphorylated GSK3β (Ser^9) cellular ELISA assay. This assay was based on a previously described protocol (33). Cells were plated in 96-well microplates at 16,000 per well

Published OnlineFirst April 27, 2010; DOI: 10.1158/1535-7163.MCT-09-0986

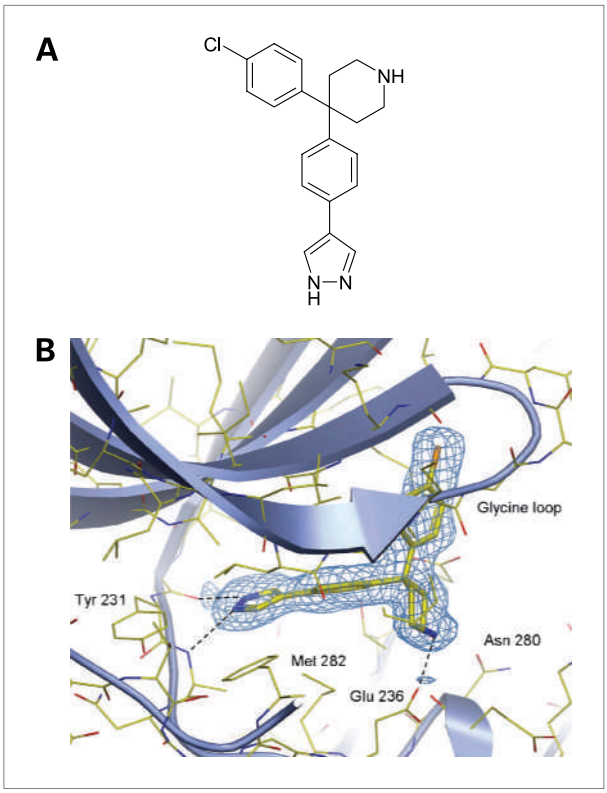

Figure 1. Structure of AT7867. A, chemical structure of AT7867. B, X-ray structure of AT7867 bound to the ATP binding site of AKT2.

in medium supplemented with 10% fetal bovine serum and grown for 24 hours before treatment with AT7867. AT7867 or vehicle control was added to the cells for 1 hour. Following this, cells were fixed with 3% paraformaldehyde, 0.25% glutaraldehyde, 0.25% Triton-X100, washed, and blocked with 5% milk in TBS with 0.1% Tween 20 before overnight incubation with a phosphorylated GSK3β (Ser^{9}) antibody (Cell Signaling Technology). The plates were then washed, secondary antibody was added, and enhancement of the signal was done using DELFIA reagents (Perkin-Elmer) as stated in the manufacturer's instructions. Europium counts were normalized to the protein concentration, and the IC_{50} value for each inhibitor was calculated in GraphPad Prism using nonlinear regression analysis and a sigmoidal dose-response (variable slope) equation.

Protein immunoblotting and immunoassay. Floating and adherent cells were collected, washed with ice-cold PBS, and harvested; lysates were prepared; and protein estimations were done as described previously (34). Samples were separated by SDS-PAGE and transferred to 0.45 μm Immobilon-P transfer membrane (Millipore). The membranes were blocked for 1 hour in blocking solution (5% milk in TBS with 0.1% Tween 20) before incubating at 4°C, shaking overnight in the following antibodies diluted in blocking solution: AKT, phosphorylated AKT (Ser^{473}), phosphorylated GSK3β (Ser^{9}), phosphorylated S6RP ($Ser^{240/244}$), FKHR, cleaved poly(ADP-ribose) polymerase (PARP; Asp^{214}) all at 1:1,000, S6 ribosomal protein at 1:2,000, phosphorylated S6RP ($Ser^{235/236}$) at 1:10,000, phosphorylated FKHR (Thr^{24})/FKHRL1 (Thr^{32}) at 1:500 (all purchased from Cell Signaling Technology), GSK3β at 1:1,000 (BD Biosciences), cyclin D1 Ab-1 (DCS-6) at 1:1,000 (NeoMarkers, Lab Vision), and glyceraldehyde-3-phosphate dehydrogenase (GAPDH) at $1:2 \times 10^{6}$ (Chemicon International, Millipore). The membranes were washed before incubation in goat anti-rabbit (1:1,000 or 1:5,000) or anti-mouse (1:10,000) horseradish peroxidase–conjugated secondary antibody for 1 hour at room temperature. Bands were visualized with ECL Western Blotting Detection Reagents and developed using Hyperfilm (GE Healthcare).

For the electrochemiluminescent immunoassay, the Meso Scale Discovery (MSD) platform was used. Cell lysates were prepared as described and probed for phosphorylation of Ser^{473} AKT, Ser^{9} GSK3β, $Ser^{235/236}$ S6RP, and total forms of AKT, GSK3β, and S6RP according to the manufacturer's instructions. Analysis was completed as recommended by the manufacturer (33, 35, 36).

Annexin V staining. U87MG cells were plated in six-well plates at 2×10^{5} per well in 2 mL growth media and grown for 24 hours before treatment. Inhibitor or DMSO was added at the specified concentrations. After the respective treatment times, adherent and floating cells were collected and washed in PBS by centrifugation. Cells were then washed in Annexin V–binding buffer

Table 1. Activity of AT7867 against selected kinases as determined by *in vitro* kinase assays

Kinase	IC_{50} (nmol/L)
AKT1	32
AKT2	17
AKT3	47
PKA	20
p70S6K	85
RSK1	>100
CDK2	>1,000
GSK3β	>1,000
c-SRC	>1,000
CHK1	>1,000
EGFR	>1,000
FGFR3	>1,000
MEK1	>1,000
PDK1	>1,000
PI3K-β	>1,000
PLK3	>1,000
RET	>1,000
SGK	>1,000
TIE2	>1,000

Published OnlineFirst April 27, 2010; DOI: 10.1158/1535-7163.MCT-09-0986

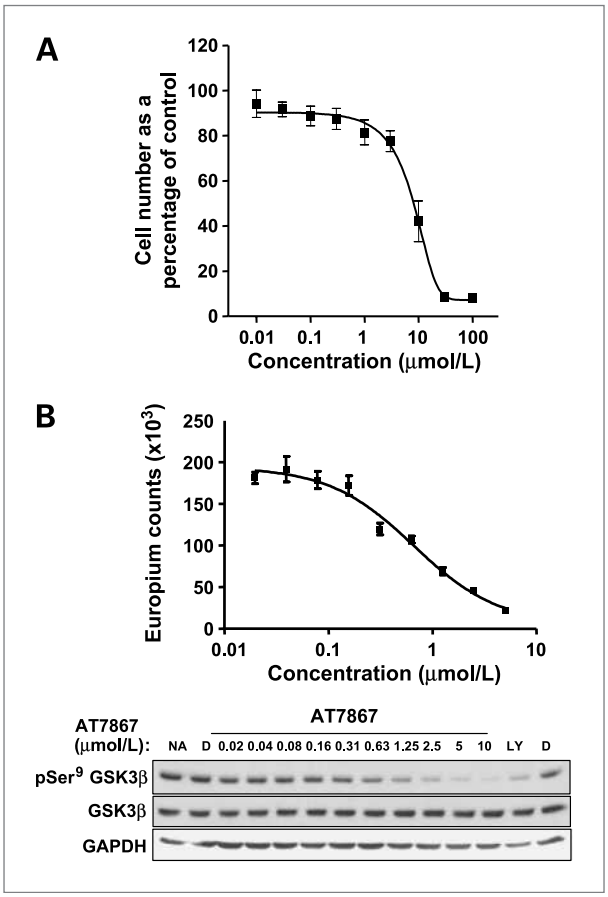

Figure 2. AT7867 inhibits proliferation of human cancer cell lines and reduces phosphorylation of GSK3β. A, PTEN-negative U87MG human glioblastoma cells were treated with a range of concentrations of AT7867 for 72 hours. Alamar blue cell viability assays were done to measure cell growth inhibition. B, cells were incubated with a range of concentrations of AT7867 for 1 hour, and the in-cell phosphorylated GSK3β ELISA was done in parallel with Western blot of cell lysates in U87MG cells. No addition (NA) and DMSO (D) vehicle were used as negative controls, and LY294002 (20 μmol/L; LY) was used as a positive control.

(10 mmol/L HEPES, 140 mmol/L NaCl, 2.5 mmol/L $CaCl_2$), resuspended in 10 μg/mL Annexin V solution, and incubated at room temperature for 15 minutes. Immediately before reading on a FACSCalibur flow cytometer, 10 μg/mL propidium iodide were added to the cell mix.

Pharmacokinetic studies. Male athymic BALB/c mice (nu/nu) were obtained from Harlan and allowed access to food and water *ad libitum*. The care and treatment of experimental animals were in accordance with the United Kingdom Coordinating Committee for Cancer Research guidelines (37).

A single dose of AT7867 was given to BALB/c mice at 5 mg/kg i.v. and 20 mg/kg p.o. Compound was formulated in a vehicle containing 10% DMSO, 20% water, and 70% hydroxypropyl-β-cyclodextrin (25% aqueous, w/v). Plasma samples were collected from duplicate animals at each of the following time points: at 0.083, 0.167, 0.33, 0.67, 1, 2, 4, 6, 16, and 24 hours after i.v. dosing and at 0.25, 0.5, 1, 2, 4, 6, and 24 hours after p.o. dosing. Mice were bled by cardiac puncture, and all blood samples were centrifuged to obtain plasma, which was then frozen at −20°C until analysis. For bioanalysis, all plasma samples were prepared by protein precipitation with acetonitrile containing internal standard. Quantification of sample extracts was, by comparison with a standard calibration line, constructed with AT7867 and using an inhibitor-specific liquid chromatography tandem mass spectrometry method. Pharmacokinetic parameters were determined using WinNonLin software.

In vivo *tumor studies.* Human MES-SA uterine sarcoma cells or U87MG human glioblastoma cells were injected s.c. in the right flank of each animal. Animals were randomized, and treatment was started with vehicle or AT7867 when established tumors were ~100 mm^3 in mean volume. Control mice received vehicle only (10% DMSO, 90% saline), and treated mice received 20 mg/kg AT7867 i.p. or 90 mg/kg AT7867 p.o. once every 3 days. Tumor size and body weight were monitored three times a week. Tumor size was evaluated by measurement with digital calipers, and changes in tumor volume in treated mice (T) versus control mice (C) are given as T divided by C (T/C ratios).

To assess the pharmacokinetic and pharmacodynamic profile, a single dose of AT7867 (90 mg/kg p.o. or 20 mg/kg i.p.) was given to mice bearing MES-SA tumor xenografts. Compound was formulated in vehicle containing 0.1% Tween 20. Plasma and tumor samples were harvested at 2, 6, and 24 hours after dosing. Mice were bled by cardiac puncture, and plasma samples were collected and frozen at −20°C until analysis. Tumors were dissected and divided into two approximately equal pieces. One piece was frozen at −20°C until pharmacokinetic analysis, whereas the other was snap frozen in liquid nitrogen until pharmacodynamic analysis. For pharmacokinetic bioanalysis, all tissue samples were first homogenized in five volumes (w/v) of acetonitrile/water (50:50). AT7867 was extracted from plasma and tissue homogenates and quantified as described

Table 2. Inhibition of cell growth across a panel of human cell lines from various tumor types; IC_{50} values are shown as the mean (n = 3) with SEM

Cell line	Cancer type	Proliferation IC_{50} ± SEM (μmol/L)
MES-SA	Uterine	0.94 ± 0.14
MDA-MB-468	Breast	2.26 ± 0.54
MCF-7	Breast	1.86 ± 0.09
U87MG	Glioma	8.22 ± 1.15
PC-3	Prostate	10.37 ± 0.79
DU145	Prostate	11.86 ± 0.67
HCT116	Colon	1.76 ± 0.36
HT29	Colon	3.04 ± 0.45

Published OnlineFirst April 27, 2010; DOI: 10.1158/1535-7163.MCT-09-0986

Table 3. A panel of human tumor cell lines were exposed to AT7867, the in-cell phosphorylated GSK3β ELISA was done, and the IC_{50} for phosphorylated Ser^9 GSK3β signal was determined

Cell line	Cancer type	$pSer^9$ GSK3β ELISA IC_{50} ± SEM (μmol/L)
MES-SA	Uterine	2.31 ± 0.61
MDA-MB-468	Breast	4.45 ± 1.47
MCF-7	Breast	2.78 ± 1.34
U87MG	Glioma	2.08 ± 0.28
PC-3	Prostate	2.65 ± 0.79
DU145	Prostate	3.21 ± 0.28
HCT116	Colon	3.3 ± 0.46
HT29	Colon	3.09 ± 1.46

above. For pharmacodynamic studies, tumors were ground to a powder under liquid nitrogen, lysed, and centrifuged to remove debris. Protein content was analyzed using bicinchoninic acid reagent, and samples run on Western blots as described above.

Results

Identification of a potent ATP-competitive inhibitor of AKT. AT7867 was discovered using fragment-based screening combined with structure-based design and was previously called compound **8a** by Saxty et al. (31). The molecule is a pyrazole, linked via the 4-position to a geminally substituted 4,4-biaryl piperidine, with the terminal aromatic group incorporating a *para*-chloro substituent (Fig. 1A). The compound is further distinguished by its relatively low molecular weight of 337 Da. For the first time, we report here the detailed biological activity of AT7867. This compound exhibited nanomolar potency toward all three AKT isoforms using isolated enzyme assays (Table 1). AT7867 also displayed potent activity against the structurally related AGC kinases p70S6K and PKA but showed a clear window of selectivity against kinases from other kinase subfamilies (Table 1).

The inhibition of AKT2 by AT7867 was shown to be ATP-competitive with a Ki of 18 nmol/L. Binding at the ATP site was confirmed by determining the three-dimensional structure of the AT7867-AKT2 complex using X-ray crystallography (Fig. 1B). The structure revealed that AT7867 fulfills a three-point pharmacophore required for potent binding to AKT2, forming hydrogen bonding interactions with the kinase hinge region, electrostatic interactions with the ribose site, and hydrophobic contacts with a lipophilic pocket in the glycine-rich loop. Specifically, the pyrazole makes a bidentate interaction with the hinge, forming hydrogen bonds with the backbone carbonyl of Glu 230 and the amide nitrogen of Ala 232. The central phenyl ring is slightly twisted with respect to the pyrazole and is sandwiched between the hydrophobic side chains of Val 166 and Met 282, which form the top and bottom of the ATP cleft. The ribose binding site is occupied by the piperidine ring, wherein the basic nitrogen forms electrostatic and hydrogen bonding interactions with the side chain of Glu 236, and the backbone carbonyl of Glu 279. The final element of the AKT-pharmacophore is fulfilled by the chlorophenyl, which is directed toward a lipophillic pocket formed by the side chains of Lys 181 and Leu 183 and the face of the glycine-rich loop in the region of Gly 161 and Gly 164.

AT7867 inhibits AKT activity in cells. *In vitro* growth inhibition studies showed that AT7867 blocked proliferation in a number of human cancer cell lines (Fig. 2A; Table 2). These cell lines represent common cancers that have been reported to exhibit deregulation of the PI3K/AKT pathway by mechanisms, such as *PTEN* or *PIK3CA* mutations. AT7867 seemed to be most potent at inhibiting proliferation in MES-SA uterine, MDA-MB-468 and MCF-7 breast, and HCT116 and HT29 colon lines (IC_{50}, 0.9–3 μmol/L) and least effective in the two prostate lines tested (IC_{50}, 10–12 μmol/L), as indicated in the figure.

The U87MG glioblastoma cell line is PTEN-deficient and exhibits a high level of phosphorylation of Ser^{473} on AKT (38), suggesting an overactive AKT pathway. This cell line has previously been used to investigate the cellular properties of several PI3K pathway inhibitors (35, 36, 39–41). For these reasons, further detailed investigations were done using U87MG cells.

The ability of AT7867 to inhibit AKT activity in human tumor cells was measured by investigating the phosphorylation state of the direct downstream substrate GSK3β following a 1-hour incubation with compound (Fig. 2B). For accurate quantification of AKT inhibition activity in cells, a 96-well plate–based ELISA was established, which allowed quantification of the level of phosphorylation of GSK3β at Ser^9 in intact cells. Figure 2B shows Western blot data and the corresponding IC_{50} data generated using the cell-based ELISA. The assay was transferable between cell lines, thus allowing the quantification of AT7867 activity in multiple lines. These experiments showed that AT7867 was equipotent at inhibiting phosphorylation of GSK3β across all cancer cell lines tested with IC_{50} values in the range of 2 to 4 μmol/L (Table 3).

Investigation of additional AKT pathway components showed that a 1-hour treatment of the U87MG cell line with AT7867 induced effects on the levels of a number of cellular proteins in a concentration-dependent fashion (Fig. 3A). This included the phosphorylation of the following AKT direct substrates: GSK3β, proapoptotic transcription factors FKHR (FoxO1a) and FKHRL1 (FoxO3a), and the downstream target S6RP. Expression of the cell cycle protein cyclin D1 was also measured. In addition to the decrease in phosphorylation of downstream substrates and a decrease in expression of cyclin D1,

Published OnlineFirst April 27, 2010; DOI: 10.1158/1535-7163.MCT-09-0986

there was an induction of AKT phosphorylation at Ser^{473}. However, at higher concentrations of compound, phosphorylation on AKT itself was also inhibited.

An additional study investigating the cellular consequences over time of AKT inhibition was also carried out. This confirmed the loss of phosphorylation on the direct AKT substrates GSK3β, FKHR, and FKHRL, as well as on the downstream target S6RP (Fig. 3B). Between 1 and 8 hours, there was a substantial loss of all phosphorylation signals under investigation. This inhibition was sustained together with loss of total proteins at 24 hours in the presence of AT7867. Loss of cyclin D1 expression

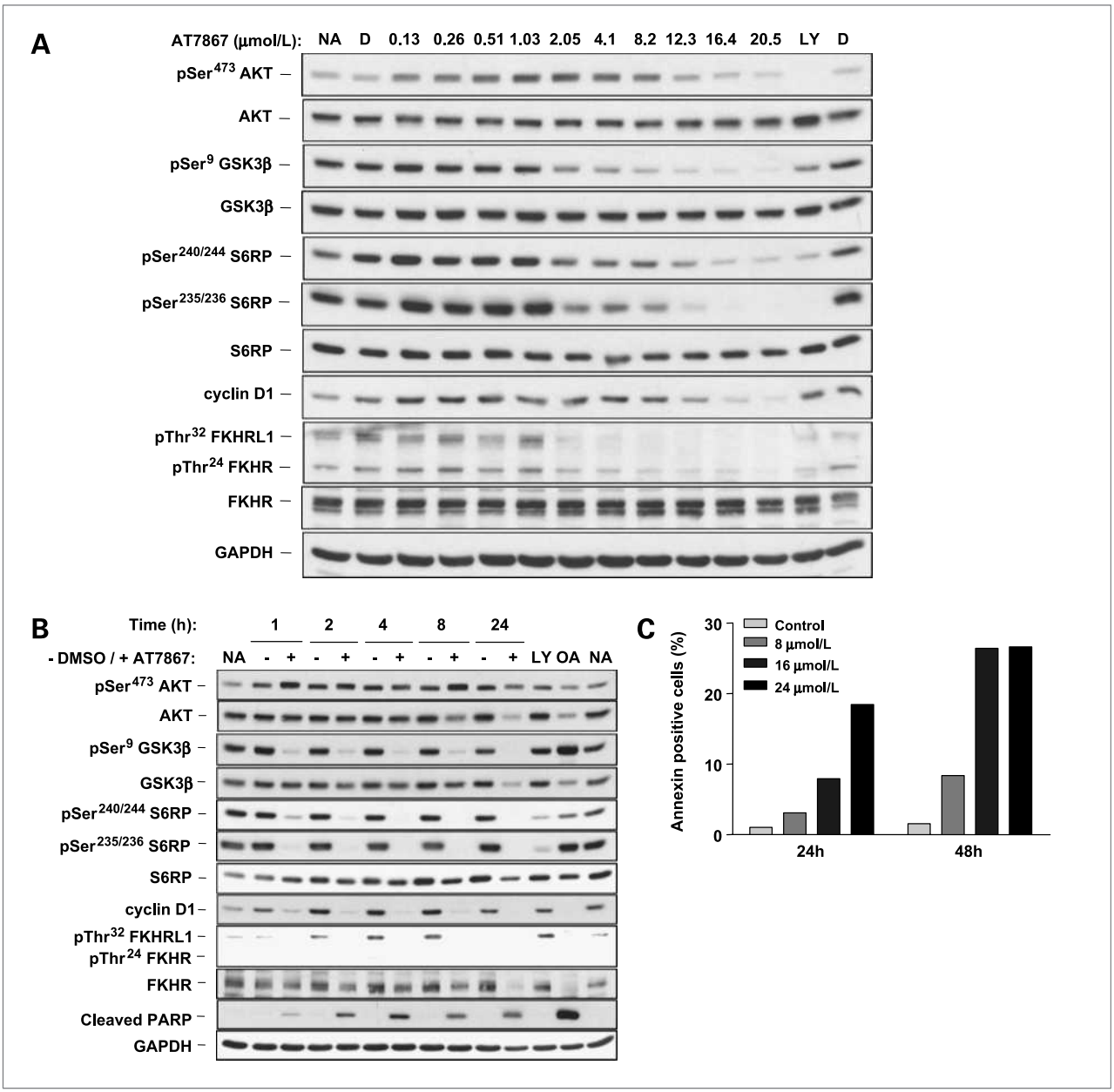

Figure 3. AT7867 suppresses AKT signaling in U87MG human glioblastoma cells in a concentration-dependent and time-dependent manner and induces apoptosis. A, PTEN-negative U87MG human glioblastoma cells were incubated with AT7867 for 1 hour, and Western blot analyses were done to assess the phosphorylation and expression of AKT pathway proteins. GAPDH was used as a loading control. No addition (NA) and DMSO (D) vehicle were used as negative controls, and LY294002 (20 μmol/L; LY) was used as a positive control. B, U87MG cells were treated with 16 μmol/L AT7867 for, 1, 2, 4, 8, and 24 hours, and Western blot analyses were done for AKT pathway proteins as indicated and the appearance of cleaved PARP. GAPDH was used as a loading control. No addition (NA) and DMSO (D) vehicle were used as negative controls, and LY294002 (20 μmol/L; LY) was used as a positive control. Okadaic acid (100 nmol/L) for 24 hour (OA) was used as a positive control for apoptosis. C, Annexin V staining of U87MG cells following treatment with 8, 16, or 24 μmol/L AT7867 or DMSO vehicle (Control) for 24 or 48 hours.

Published OnlineFirst April 27, 2010; DOI: 10.1158/1535-7163.MCT-09-0986

was seen at 1 hour posttreatment and was maintained over the 24-hour period of the experiment, at which time the amount of AKT pathway proteins was reduced to below control levels. Because loss of phosphorylation on the proapoptotic proteins FKHR and FKHRL allows their entry into the nucleus to facilitate gene transcription leading to activation of apoptosis, the effect of AT7867 on apoptosis was studied (16). Cleavage of the protein PARP is an event that occurs early in the apoptotic process, and as such, cleaved PARP serves as a marker of cells undergoing apoptosis (42). The appearance of cleaved PARP was observed in cells exposed to AT7867 from 1 hour onwards for the duration of the study and correlated with the reduction in protein levels described above for the pathway components (Fig. 3B). Apoptosis was further investigated by Annexin V staining, which detects phosphatidylserine on the external surface of intact cells, another hallmark of apoptosis (43). A concentration-dependent and time-dependent increase in the amount of Annexin V staining was observed (Fig. 3C).

In view of the effects of AT7867 on AKT and p70S6K, the MSD electrochemiluminescent immunoassay platform was used to quantify the inhibitory effects of this compound on the phosphorylation of GSK3β, p70S6K, and S6RP following AT7867 treatment in U87MG glioblastoma cells (Table 4). At 1 hour posttreatment, the IC_{50} for $pSer^{9}$ GSK3β was 7.1 μmol/L. An IC_{50} value could not, however, be obtained for $pThr^{421/424}$ of p70S6K, as it was greater than the maximal concentration of AT7867 used in the assay (20 μmol/L). In contrast, IC_{50} values of 10.7 and 12.3 μmol/L were obtained for $pSer^{235/236}$ and $pSer^{240/244}$ of S6RP.

In vivo *activity of AT7867.* Having shown concentration-dependent and time-dependent effects of AT7867 *in vitro*, the properties of the compound were evaluated *in vivo* in mice. The plasma clearance of AT7867 following 5 mg/kg i.v. administration was moderate, and the compound was still detectable in plasma at 24 hours post-administration (Fig. 4A). Following p.o. administration at 20 mg/kg, the elimination of AT7867 from plasma seemed to be similar to that observed after i.v. administration (Fig. 4A). Plasma levels of AT7867 remained above 0.5 μmol/L for at least 6 hours following a p.o.

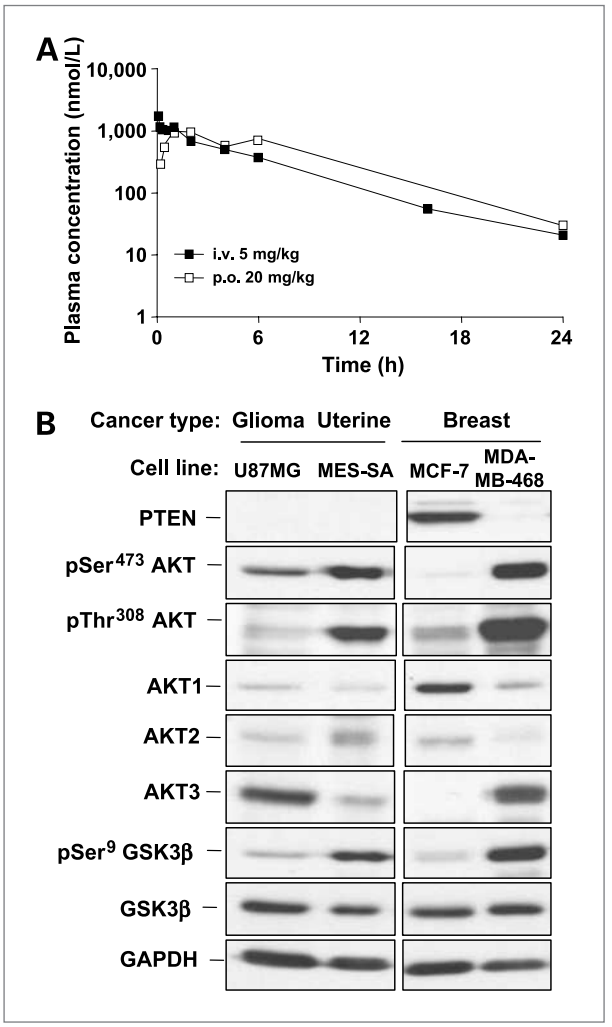

Figure 4. The plasma pharmacokinetic profile of AT7867 *in vivo* and comparison of expression of AKT pathway proteins in the MES-SA human uterine versus U87MG glioblastoma and MCF-7 and MDA-MB-468 breast cell lines. A, plasma pharmacokinetic in mice following administration of AT7867 at 20 mg/kg p.o. and 5 mg/kg i.v. B, Western blot analysis of AKT pathway proteins in lysates prepared from MES-SA, U87MG, MCF7, and the MDA-MB-468 cell lines. GAPDH was used as a loading control.

Table 4. U87MG cells were treated with 0.1 to 20 μmol/L AT7867 for 1 h; lysates were prepared, and analysis of AKT pathway proteins was done by electrochemiluminescent immunoassay (MSD) as indicated

IC_{50} (μmol/L)	GSK3β $pSer^{9}$	P70S6K $pThr^{421}$/ Ser^{424}	S6RP $pSer^{235/236}$	S6RP $pSer^{240/244}$
AT7867	7.1	>20	10.7	12.3

dose of 20 mg/kg. Assuming linear pharmacokinetics following i.v. administration, the bioavailability by the p.o. route was calculated to be 44%.

From *in vitro* cell growth studies, the MES-SA uterine cell line seemed to be the most sensitive to growth inhibition by AT7867. This cell line does not express PTEN and contains high levels of phosphorylated AKT, indicating an overactive pathway (Fig. 4B). *In vivo* pharmacodynamic biomarker studies were therefore done with this model. Following pharmacokinetic (see above) and tolerability studies, doses of AT7867 (90 mg/kg p.o. or 20 mg/kg i.p.) were given to athymic mice bearing MES-SA tumors, and the phosphorylation status of GSK3β and S6RP in tumors was monitored

Published OnlineFirst April 27, 2010; DOI: 10.1158/1535-7163.MCT-09-0986

over time. Clear inhibition of phosphorylation of the two markers of pathway activity was seen at 2 and 6 hours following treatment with AT7867 (Fig. 5A and B). By 24 hours, total levels of both GSK3β and S6RP were greatly reduced, as also seen in the *in vitro* studies. For both routes of administration and at each time point investigated, the level of compound in the plasma and tumor exceeded the cellular IC_{50}, which was consistent with the prolonged mechanistic biomarker effect (Fig. 5C and D). As seen in studies *in vitro*, sustained compound exposure induced an increase in cleaved PARP, indicating that AT7867 also induces apoptosis in the xenograft tumor cells (Fig. 5A and B).

Next we determined the effect of AT7867 on the growth of MES-SA tumor xenografts. Marked inhibition of tumor growth, as assessed by changes in volume, were seen with this model when dosed at the same levels and routes as used for the pharmacodynamic studies described above. Specifically, a T/C of 0.37 was observed at 20 mg/kg i.p. (measured at the termination of the experiment on day 12; Fig. 6A), and a T/C of 0.38 was observed at 90 mg/kg p.o. (measured on day 10; Fig. 6B). Additional *in vivo* xenograft studies were carried out using the U87MG cell line, which was sensitive to the effects of AT7867 *in vitro*, although less so than the MES-SA cell line. Figure 6C shows a T/C of 0.51 (measured on day 13), when 20 mg/kg AT7867 was dosed on this schedule via the i.p. route of administration.

Discussion

AKT activity has been implicated in the regulation of tumor cell growth, proliferation, metastasis, and apoptosis (1). Recently, the PI3K/AKT signal transduction pathway has become the focus of intense interest as a critical regulator of tumor cell survival, and a number

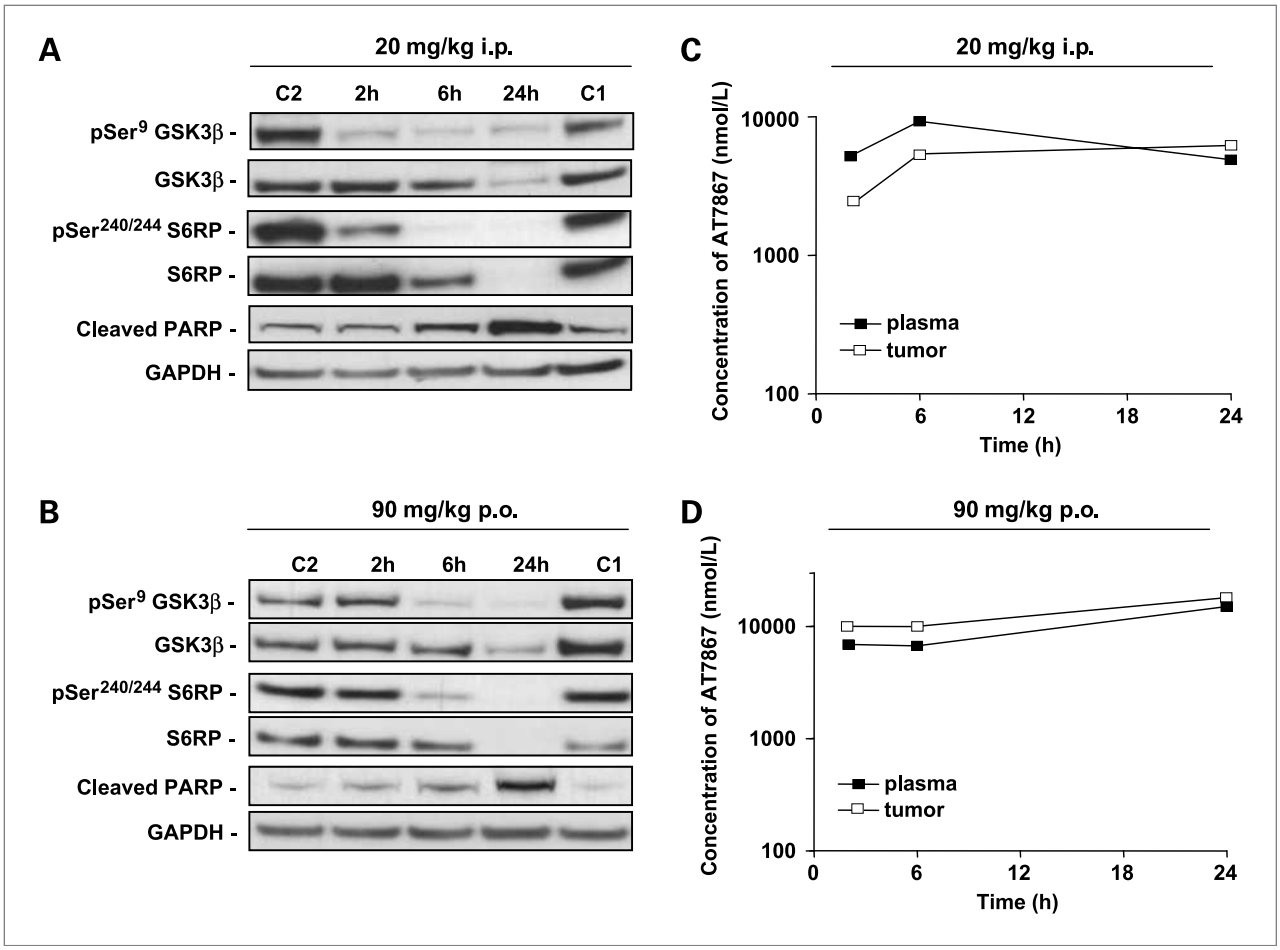

Figure 5. The pharmacodynamic and pharmacokinetic profiles of AT7867. Athymic BALB/c mice bearing MES-SA human uterine xenograft tumors were treated with a single dose of AT7867 at 20 mg/kg i.p. and 90 mg/kg p.o. Plasma and tumors were harvested at 2, 6, or 24 hours after dosing. A and B, phosphorylated and total GSK3β, S6RP, cleaved PARP, and GAPDH were assessed from tumor protein lysates by Western blotting at each dose as indicated. C1, control 1; C2, control 2. C and D, plasma and tumor concentrations of AT7867 were assessed by liquid chromatography tandem mass spectrometry at each dose as indicated.

Published OnlineFirst April 27, 2010; DOI: 10.1158/1535-7163.MCT-09-0986

of AKT pathway inhibitors have been disclosed with a wide variety of potencies and specificities (2, 44, 45). In this report, we describe the *in vitro* and *in vivo* effects of AT7867, a recently developed inhibitor of AKT and p70S6K, which has been identified using fragment-based lead discovery and structure-based design technologies (29–32).

AT7867 is a potent inhibitor of AKT and p70S6K that blocks the cellular phosphorylation of the AKT substrate GSK3β and the p70S6K substrate S6RP and inhibits the proliferation of a range of human tumor cell lines. It is interesting to note that, whereas the IC_{50} for growth inhibition varied 12-fold (1–12 μmol/L), the IC_{50} for GSK3β phosphorylation was much more consistent (2–4.5 μmol/L) across the same cell line panel. This discrepancy is perhaps not surprising because the response of different cell lines to the same level of pathway inhibition may be dependent on factors other than genetic alterations on the PI3K/AKT pathway. Further detailed studies in the PTEN-deficient human glioblastoma U87MG cell line showed that AT7867 caused both a concentration-dependent and time-dependent reduction in the phosphorylation of proteins downstream of AKT, including the AKT substrate GSK3β and p70S6K target S6RP. Cyclin D1 expression and thus cell cycle progression is regulated at the post-translational level by GSK3β and also by protein translation through p70S6K via mTOR (12). The demonstration that AT7867 suppresses the expression of cyclin D1 is consistent with growth inhibition being mediated via these kinases. Induction of phosphorylation on AKT itself at Ser^{473} was also noted, consistent with the compensatory but futile feedback regulation of AKT previously described with other inhibitors of this pathway (46–48).

Growing evidence has challenged the view of a linear PI3K/AKT/mTOR pathway, with the identification of cross-talk and feedback regulation within the pathway (8, 18). Despite induction of $pSer^{473}$ AKT, the phosphorylation of downstream AKT targets was markedly decreased in the presence of AT7867 both in cancer cell lines *in vitro* and human tumor xenografts in immunosuppressed mice. Recent papers have suggested that dual inhibition of PI3K and mTOR could overcome these feedback mechanisms through vertical blockade of key components of the pathway (35, 41, 49). AT7867 has little activity outside the AGC kinase family members but is a potent inhibitor of the structurally related AGC kinases PKA and p70S6K, as well as AKT. To dissect the respective contributions of AKT and p70S6K inhibition along this pathway to AT7867-mediated effects, the relative modulation in substrate phosphorylation signals were quantified in U87MG cells. Whereas the IC_{50} for $pSer^{9}$ GSK3β was 7.1 μmol/L, an IC_{50} value could not be generated for p70S6K, as it was greater than the highest concentration of 20 μmol/L used in this assay. This suggests a dilution of the inhibition of the pathway signal, as p70S6K is more distal than GSK3β from the AKT target. In contrast, IC_{50} values were obtained for both $pSer^{235/236}$ and $pSer^{241/244}$ of S6RP of 10.7 μmol/L and 12.3 μmol/L, respectively con-

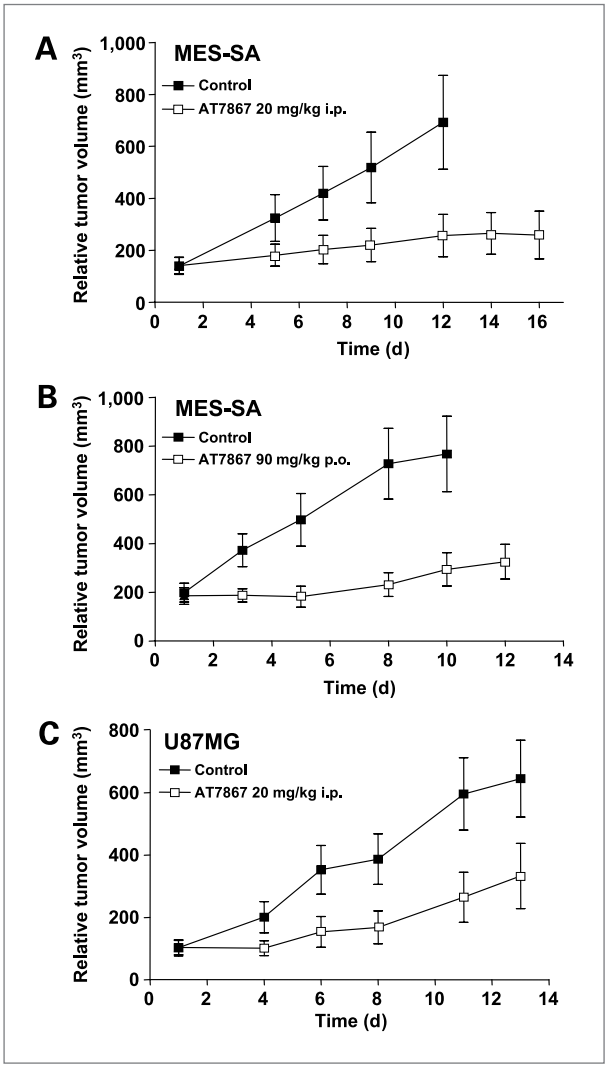

Figure 6. AT7867 suppresses MES-SA human uterine and U87MG human glioblastoma xenograft tumor growth. A, athymic BALB/c mice bearing MES-SA xenograft tumors were given AT7867 20 mg/kg i.p. once every 3 days for 16 days. B, athymic BALB/c mice bearing MES-SA xenograft tumors were given AT7867 at 90 mg/kg p.o. once every 3 days for 12 days. C, athymic BALB/c mice bearing U87MG xenograft tumors were given AT7867 at 20 mg/kg i.p. once every 3 days for 13 days. Tumor size was monitored three times a week, and relative tumor volumes were calculated.

firming the direct inhibitory effects of AT7867 against p70S6K. It is an intriguing possibility that the combined effects of targeting p70S6K and AKT with this compound may serve to improve its therapeutic potential by delivering a double vertical blockade to the pathway.

It should be noted that, based on kinase profiling in *in vitro* biochemical assays, it is possible that inhibition of PKA may contribute to the cellular effects of AT7867. However, as there are no suitable methods or reagents that can accurately dissect the specific effects of PKA on its target substrates in the cell lines used, this possibility could not be pursued at this time. Further studies are

Published OnlineFirst April 27, 2010; DOI: 10.1158/1535-7163.MCT-09-0986

also needed to profile the potential effects of AT7867 on other signaling pathways, and gene expression profiling studies using cDNA microarray are now under way to address this in an unbiased fashion.

A major function of AKT in cancer cells is to prevent apoptosis by the phosphorylation and inactivation of proapoptotic targets, such as the forkhead transcription factors and BAD (50). We have shown that AT7867 prevents phosphorylation of FKHR and FKHRL1 and inhibits tumor cell growth, an effect that may in part be attributed to the induction of apoptosis caused by the compound. The proapoptotic effect of AT7867 is supported by the induction of cleaved PARP and Annexin V staining in treated cells, which correlated with the reduction in protein levels for PI3K/AKT pathway components at later time points (Fig. 3B).

Although the PI3K/AKT pathway has often been associated with survival signaling and apoptosis (1), there has been equivocal evidence in support of this hypothesis from studies involving the pharmacologic ablation of key components of this key signaling cascade. We have previously shown that the potent and selective class I PI3K and mTOR inhibitor PI-103 does not cause significant apoptosis in a wide range of tumor cell lines tested (35, 41). In contrast, we have shown here that AT7867 results in extensive apoptosis, both *in vitro* and *in vivo*, suggesting a difference in the simultaneous effects of inhibiting both AKT and p70S6K versus PI3K and mTOR. These data suggest that there may be unknown mechanisms resulting in this vital difference in survival signaling, with the possibility of cross-talk or other undiscovered pathway proteins playing a key role. Also, the results suggest that combined inhibitors of AKT and p70S6K may potentially be efficacious as monotherapy.

Pharmacokinetic studies showed that potentially active concentrations of AT7867 could be achieved in plasma and tumor after 20 mg/kg i.p. or 90 mg/kg p.o. reflecting the relatively high oral bioavailability of this compound. The *in vitro* pharmacodynamic biomarker effects of AT7867 described above were also observed in tumor models *in vivo*. Administration of AT7867 p.o. or i.p. to mice bearing human tumor xenografts caused suppression of phosphorylation of the AKT and p70S6K molecular biomarkers GSK3β and S6RP and a concomitant increase in the levels of cleaved PARP. These pharmacodynamic effects were achieved at plasma and tumor drug concentrations similar to those required to suppress the same markers *in vitro* and at doses that cause inhibition of human tumor xenograft growth (Fig. 6A–C). Therefore, these data are consistent with inhibition of AKT and p70S6K as the mechanism of tumor growth suppression for AT7867 *in vivo*.

In conclusion, we have shown that AT7867 suppresses tumor cell proliferation, induces apoptosis, and exhibits oral antitumor activity. Importantly, we show that AT7867 suppresses the phosphorylation of downstream markers of AKT and p70S6K in tumor tissue at doses that also inhibit human xenograft tumor growth. The therapeutic response to AKT and p70S6K pathway inhibition observed in the current study makes this approach attractive for clinical application, wherein such a novel inhibitor of both AKT and p70S6K may have the potential to cause antitumor activity as a single agent or in combination with other agents.

Disclosure of Potential Conflicts of Interest

K.M. Grimshaw, S.J. Woodhead, T.G. Davies, L. Fazal, M. Reule, L.C. Seavers, V. Lock, J.F. Lyons, and N.T. Thompson: current or former employees of Astex Therapeutics, which has a commercial interest in the development of AKT inhibitors, including AT7867. L-J.K. Hunter, T.A. Yap, S.P. Heaton, M.I. Walton, P. Workman, and M.D. Garrett: current or former employees of The Institute of Cancer Research, which also has a commercial interest in the development of AKT inhibitors, including AT7867, and operates a rewards for inventors scheme. Both Astex Therapeutics and The Institute of Cancer Research have been involved in a commercial collaboration with Cancer Research Technology Limited to discover and develop inhibitors of AKT and intellectual property arising from this program has been licensed to AstraZeneca.

Grant Support

Cancer Research UK grants C309/A8274 (L-J.K. Hunter, T.A. Yap, M.I. Walton, P. Workman, and M.D. Garrett) and C51/A7401 (through the Experimental Cancer Medicine Centre network initiative; S.P. Heaton), The Institute of Cancer Research (M.D. Garrett), and Astex Therapeutics (L-J.K. Hunter). We acknowledge NHS funding to the NIHR Biomedical Research Centre.

The costs of publication of this article were defrayed in part by the payment of page charges. This article must therefore be hereby marked *advertisement* in accordance with 18 U.S.C. Section 1734 solely to indicate this fact.

Received 10/23/2009; revised 02/23/2010; accepted 02/26/2010; published OnlineFirst 04/27/2010.

References

1. Vivanco I, Sawyers CL. The phosphatidylinositol 3-kinase AKT pathway in human cancer. Nat Rev Cancer 2002;2:489–501.
2. Yap TA, Garrett MD, Walton MI, Raynaud F, de Bono JS, Workman P. Targeting the PI3K-AKT-mTOR pathway: progress, pitfalls, and promises. Curr Opin Pharmacol 2008;8:449–557.
3. Bellacosa A, Kumar CC, Di Cristofano A, Testa JR. Activation of AKT kinases in cancer: implications for therapeutic targeting. Adv Cancer Res 2005;94:29–86.
4. Alessi DR, Andjelkovic M, Caudwell B, et al. Mechanism of activation of protein kinase B by insulin and IGF-1. EMBO J 1996;15:6541–51.
5. Alessi DR, James SR, Downes CP, et al. Characterization of a 3-phosphoinositide-dependent protein kinase which phosphorylates and activates protein kinase Bα. Curr Biol 1997;7:261–9.
6. Stokoe D, Stephens LR, Copeland T, et al. Dual role of phosphatidylinositol-3,4,5-trisphosphate in the activation of protein kinase B. Science 1997;277:567–70.
7. Sarbassov DD, Guertin DA, Ali SM, Sabatini DM. Phosphorylation and regulation of Akt/PKB by the rictor-mTOR complex. Science 2005;307:1098–101.
8. Balendran A, Casamayor A, Deak M, et al. PDK1 acquires PDK2 activity in the presence of a synthetic peptide derived from the carboxyl terminus of PRK2. Curr Biol 1999;9:393–404.

Published OnlineFirst April 27, 2010; DOI: 10.1158/1535-7163.MCT-09-0986

9. Persad S, Attwell S, Gray V, et al. Regulation of protein kinase B/Akt-serine 473 phosphorylation by integrin-linked kinase: critical roles for kinase activity and amino acids arginine 211 and serine 343. J Biol Chem 2001;276:27462–9.
10. Feng J, Park J, Cron P, Hess D, Hemmings BA. Identification of a PKB/Akt hydrophobic motif Ser-473 kinase as DNA-dependent protein kinase. J Biol Chem 2004;279:41189–96.
11. Maehama T, Dixon JE. The tumor suppressor, PTEN/MMAC1, dephosphorylates the lipid second messenger, phosphatidylinositol 3,4,5-trisphosphate. J Biol Chem 1998;273:13375–8.
12. Mamane Y, Petroulakis E, LeBacquer O, Sonenberg N. mTOR, translation initiation and cancer. Oncogene 2006;25:6416–22.
13. Frame S, Cohen P. GSK3 takes centre stage more than 20 years after its discovery. Biochem J 2001;359:1–16.
14. Downward J. How BAD phosphorylation is good for survival. Nat Cell Biol 1999;1:E33–5.
15. Cardone MH, Roy N, Stennicke HR, et al. Regulation of cell death protease caspase-9 by phosphorylation. Science 1998;282:1318–21.
16. Brunet A, Bonni A, Zigmond MJ, et al. Akt promotes cell survival by phosphorylating and inhibiting a Forkhead transcription factor. Cell 1999;96:857–68.
17. Carracedo A, Pandolfi PP. The PTEN-PI3K pathway: of feedbacks and cross-talks. Oncogene 2008;27:5527–41.
18. Carpten JD, Faber AL, Horn C, et al. A transforming mutation in the pleckstrin homology domain of AKT1 in cancer. Nature 2007;448:439–44.
19. Staal SP. Molecular cloning of the akt oncogene and its human homologues AKT1 and AKT2: amplification of AKT1 in a primary human gastric adenocarcinoma. Proc Natl Acad Sci U S A 1987;84:5034–7.
20. Di Cristofano A, Pandolfi PP. The multiple roles of PTEN in tumor suppression. Cell 2000;100:387–90.
21. Samuels Y, Wang Z, Bardelli A, et al. High frequency of mutations of the PIK3CA gene in human cancers. Science 2004;304:554.
22. Kim D, Dan HC, Park S, et al. AKT/PKB signaling mechanisms in cancer and chemoresistance. Front Biosci 2005;10:975–87.
23. Brognard J, Clark AS, Ni Y, Dennis PA. Akt/protein kinase B is constitutively active in non-small cell lung cancer cells and promotes cellular survival and resistance to chemotherapy and radiation. Cancer Res 2001;61:3986–97.
24. Nagata Y, Lan KH, Zhou X, et al. PTEN activation contributes to tumor inhibition by trastuzumab, and loss of PTEN predicts trastuzumab resistance in patients. Cancer Cell 2004;6:117–27.
25. LoPiccolo J, Blumenthal GM, Bernstein WB, Dennis PA. Targeting the PI3K/Akt/mTOR pathway: effective combinations and clinical considerations. Drug Resist Updat 2007;11:32–50.
26. Knight ZA, Gonzalez B, Feldman ME, et al. A pharmacological map of the PI3-K family defines a role for p110α in insulin signaling. Cell 2006;125:733–47.
27. Workman P, Clarke P, Raynaud F, van Montfort R. Drugging the PI3 kinome: from chemical tools to drugs in the clinic. Cancer Res 2010;70:2146–57.
28. Huang S, Houghton PJ. Inhibitors of mammalian target of rapamycin as novel antitumor agents: from bench to clinic. Curr Opin Investig Drugs 2002;3:295–304.
29. Yang J, Cron P, Good VM, Thompson V, Hemmings BA, Barford D. Crystal structure of an activated Akt/protein kinase B ternary complex with GSK3-peptide and AMP-PNP. Nature Structural Biology 2002;9:940–4.
30. Donald A, McHardy T, Rowlands MG, et al. Rapid evolution of 6-phenylpurine inhibitors of protein kinase B through structure-based design. J Med Chem 2007;50:2289–92.
31. Saxty G, Woodhead SJ, Berdini V, et al. Identification of inhibitors of protein kinase B using fragment-based lead discovery. J Med Chem 2007;50:2293–6.
32. Davies TG, Verdonk ML, Graham B, et al. A structural comparison of inhibitor binding to PKB, PKA and PKA-PKB chimera. J Mol Biol 2007;367:882–94.
33. Gowan SM, Hardcastle A, Hallsworth AE, et al. Application of meso scale technology for the measurement of phosphoproteins in human tumor xenografts. Assay Drug Dev Technol 2007;5:391–401.
34. Fry DW, Bedford DC, Harvey PH, et al. Cell cycle and biochemical effects of PD 0183812. A potent inhibitor of the cyclin D-dependent kinases CDK4 and CDK6. J Biol Chem 2001;276:16617–23.
35. Guillard S, Clarke PA, Te Poele R, et al. Molecular pharmacology of phosphatidylinositol 3-kinase inhibition in human glioma. Cell Cycle 2009;8:443–53.
36. Raynaud FI, Eccles SA, Patel S, et al. Biological properties of potent inhibitors of class I phosphatidylinositide 3-kinases: from PI-103 through PI-540, PI-620 to the oral agent GDC-0941. Mol Cancer Ther 2009;8:1725–38.
37. Workman P, Twentyman P, Balkwill F, et al. United Kingdom Coordinating Committee on Cancer Research (UKCCCR) guidelines for the welfare of animals in experimental neoplasia (Second Edition). Br J Cancer 1998;77:1–10.
38. Haas-Kogan D, Shalev N, Wong M, Mills G, Yount G, Stokoe D. Protein kinase B (PKB/Akt) activity is elevated in glioblastoma cells due to mutation of the tumor suppressor PTEN/MMAC. Curr Biol 1998;8:1195–8.
39. Shingu T, Yamada K, Hara N, et al. Synergistic augmentation of antimicrotubule agent-induced cytotoxicity by a phosphoinositide 3-kinase inhibitor in human malignant glioma cells. Cancer Res 2003;63:4044–7.
40. Yu K, Lucas J, Zhu T, et al. PWT-458, a novel pegylated-17-hydroxywortmannin, inhibits phosphatidylinositol 3-kinase signaling and suppresses growth of solid tumors. Cancer Biol Ther 2005;4:538–45.
41. Raynaud FI, Eccles S, Clarke PA, et al. Pharmacologic characterization of a potent inhibitor of class I phosphatidylinositide 3-kinases. Cancer Res 2007;67:5840–50.
42. Oliver FJ, de la Rubia G, Rolli V, Ruiz-Ruiz MC, de Murcia G, Murcia JM. Importance of poly(ADP-ribose) polymerase and its cleavage in apoptosis. Lesson from an uncleavable mutant. J Biol Chem 1998;273:33533–9.
43. Martin SJ, Reutelingsperger CP, McGahon AJ, et al. Early redistribution of plasma membrane phosphatidylserine is a general feature of apoptosis regardless of the initiating stimulus: inhibition by overexpression of Bcl-2 and Abl. J Exp Med 1995;182:1545–56.
44. Garcia-Echeverria C, Sellers WR. Drug discovery approaches targeting the PI3K/Akt pathway in cancer. Oncogene 2008;27:5511–26.
45. Ihle NT, Powis G. Take your PIK: phosphatidylinositol 3-kinase inhibitors race through the clinic and toward cancer therapy. Mol Cancer Ther 2009;8:1–9.
46. Han EK, Leverson JD, McGonigal T, et al. Akt inhibitor A-443654 induces rapid Akt Ser-473 phosphorylation independent of mTORC1 inhibition. Oncogene 2007;26:5655–61.
47. Luo Y, Shoemaker AR, Liu X, et al. Potent and selective inhibitors of Akt kinases slow the progress of tumors *in vivo*. Mol Cancer Ther 2005;4:977–86.
48. O'Reilly KE, Rojo F, She QB, et al. mTOR inhibition induces upstream receptor tyrosine kinase signaling and activates Akt. Cancer Res 2006;66:1500–8.
49. Fan QW, Knight ZA, Goldenberg DD, et al. A dual PI3 kinase/mTOR inhibitor reveals emergent efficacy in glioma. Cancer Cell 2006;9:341–9.
50. Song G, Ouyang G, Bao S. The activation of Akt/PKB signaling pathway and cell survival. J Cell Mol Med 2005;9:59–71.

AACR American Association for Cancer Research

Molecular Cancer Therapeutics

AT7867 Is a Potent and Oral Inhibitor of AKT and p70 S6 Kinase That Induces Pharmacodynamic Changes and Inhibits Human Tumor Xenograft Growth

Kyla M. Grimshaw, Lisa-Jane K. Hunter, Timothy A. Yap, et al.

Mol Cancer Ther 2010;9:1100-1110. Published OnlineFirst April 27, 2010.